The Effect of Interlayer Cations on the Magnetic Properties of the Mixed-Metal Pnictide Oxides: $A_2MnZn_2As_2O_2$ (A = Sr, Ba)

Tadashi C. Ozawa and Susan M. Kauzlarich*

Department of Chemistry, One Shields Avenue, University of California, Davis, California 95616

Mario Bieringer, Chris R. Wiebe, and John E. Greedan*

Institute for Materials Research, McMaster University, Hamilton, Ontario L8S 4M1, Canada

Jason S. Gardner

The Neutron Program for Materials Research, NRC, Chalk River Labs, Chalk River, Ontario K0J 1J0, Canada

Received September 14, 2000. Revised Manuscript Received December 29, 2000

The new pnictide oxide $Sr_2MnZn_2As_2O_2$ is reported. The crystal structure of this compound consists of a 1:1 intergrowth of square-planar MnO_2^{2-} layers and $ThCr_2Si_2$-type $Zn_2As_2^{2-}$ layers interspersed by Sr cations. This compound has been prepared by sintering the stoichiometric ratio of SrO, Mn, Zn, and As in a fused-silica ampule under 0.2 atm of Ar at 1000 °C for 1 week. The sample quality has been examined by Rietveld refinement of the powder X-ray diffraction data, and the transition metal site (2a and 4d) selectivity has been analyzed by Rietveld refinement of powder neutron diffraction data. Furthermore, effects of this structural order on the magnetic susceptibility and interaction between the magnetic layers have been analyzed by temperature-dependent magnetization measurements. The magnetic structures of both phases, $A_2MnZn_2As_2O_2$ (A = Sr, Ba), have been investigated by temperature-dependent powder neutron diffraction. The Ba analogue exhibits two-dimensional short-range order below about 40 K, whereas for the Sr analogue, no evidence for either long- or short-range order was found over the 2θ range investigated down to 4 K. The results of these characterizations are compared with those of the previously studied phase, $Sr_2Mn_3As_2O_2$.

Introduction

Layered transition metal oxides[1,2] are fascinating materials to investigate because of their unusual physical properties. For example, there have been extensive studies on layered high-T_c superconducting cuprates[3−6] and CMR (colossal magneto-resistance) manganites.[7−11] Recently, several mixed-metal mixed-layered oxychalcogenides[12−17] and pnictide oxides[18−20] have been investigated as part of a search for materials with undiscovered novel properties. These mixed-layer materials are interesting because the two different kinds of transition metals segregate into specific crystallographic sites within the compound in a chemically controlled manner. This control can be rationalized on the basis of the general trend in the reactivity of each

* To whom correspondence should be addressed

(1) Salvador, P. A.; Mason, T. O.; Hagerman, M. E.; Poeppelmeier, K. R. In *Chemistry of Advanced Materials: An Overview*; Interrante, L. V., Hampden-Smith, M. J., Eds.; Wiley-VCH: New York, 1998; Chapter 10, p 449.
(2) Anderson, M., T.; Vaughey, J., T.; Poeppelmeier, K. R. *Chem. Mater.* **1993**, *5*, 151.
(3) Cava, R. J. *Nature* **1993**, *362*, 204.
(4) Sleight, A. W. *Acc. Chem. Res.* **1995**, *28*, 103.
(5) Service, R. F. *Science* **1996**, *271*, 1804.
(6) Chu, P. W. *Sci. Am.* **1995**, *273*, 128.
(7) Hayashi, T.; Miura, N.; Tokunaga, M.; Kimura, T.; Tokura, Y. *J. Phys.: Condens. Matter* **1998**, *10*, 11525.
(8) Battle, P. D.; Kasmir, N.; Millburn, J. E.; Rosseinsky, M. J.; Patel, R. T.; Spring, L. E. Blundell, S. I.; Hayes, W.; Klene, A. K.; Minut, A.; Singleton, J. *J. Appl. Phys.* **1998**, *83*, 6379.
(9) Argyriou, D. N.; Kelley, T. M.; Mitchell, J. F.; Robinson, R. A.; Osborn, R.; Rosenkranz, S.; Sheldon, R. I.; Jorgensen, J. D. *J. Appl. Phys.* **1998**, *83*, 6374.
(10) Argyriou, D. N.; Mitchell, J. F.; Jorgensen, J. D.; Goodenough, J. B.; Radaelli, P. G.; Cox, D. E.; Bordallo, H. N. *Aust. J. Phys.* **1999**, *52*, 279.
(11) Mitchell, J. F.; Millburn, J. E.; Medarde, M.; Short, S.; Jorgensen, J. D.; Fernández-Díaz, M. T. *J. Solid State Chem.* **1998**, *141*, 599.
(12) Park, Y.; DeGroot, D. C.; Schinder, J. L.; Kannewurf, C. R.; Kanatzidis, M. G. *Chem. Mater.* **1993**, *5*, 8.
(13) Zhu, W. J.; Hor, P. H. *J. Solid State Chem.* **1997**, *130*, 319.
(14) Zhu, W. J.; Hor, P. H.; Jacobson, A. J.; Crisci, G.; Albright, T. A.; Wang, S. H.; Vogt, T. *J. Am. Chem. Soc.* **1997**, *119*, 12398.
(15) Zhu, W. J.; Hor, P. H. *Inorg. Chem.* **1997**, *36*, 3576.
(16) Zhu, W. J.; Hor, P. H. *J. Solid State Chem.* **1997**, *134*, 128.
(17) Otzschi, K.; Ogino, H.; Shimoyama, J.-i.; Kishio, K. *J. Low Temp. Phys.* **1999**, *117*, 729.
(18) Ozawa, T.; Olmstead, M. M.; Brock, S. L.; Kauzlarich, S. M.; Young, D. M. *Chem. Mater.* **1998**, *10*, 392.
(19) Matsushita, A.; Ozawa, T. C.; Tang, J.; Kauzlarich, S. M. *Physica B* **2000**, *284−288*, 1424.
(20) Enjalran, M.; Scalettar, R. T.; Kauzlarich, S. M. *Phys. Rev. B* **2000**, *61*, 14570.

10.1021/cm000743j CCC: $20.00
Published on Web 02/10/2001

Table 1. Crystallographic Parameters for $Sr_2MnZn_2As_2O_2$ (Space Group *I*4/*mmm*) from Rietveld Refinement[a]

	powder X-ray diffraction	powder neutron diffraction (IPNS)
a (Å)	4.126237(24)	4.122979(26)
c (Å)	18.67091(16)	18.65868(21)
2a site occupancy by Mn	N/A	0.996(4)
4b site occupancy by Zn	N/A	0.940(5)
ρ_{calc} (g cm^{-3})	5.6709(1)	5.6836(1)
χ^2	4.186	2.365
R_{wp} (%)	19.49	6.34
R_p (%)	14.53	4.33
no. of parameters	60	32
temp (K)	room temp	room temp

[a] $R_{wp} = [\Sigma(F_0^2 - SF_c^2)^2/\Sigma(wI_0^2)]^{1/2}$; $R_p = \Sigma|I_0 - I_c|/\Sigma I_0$.

Table 2. Atomic Coordinates and Displacement Coefficients (Å^2)[a] Obtained from the Rietveld Refinement of Powder Neutron Diffraction Data for $Sr_2MnZn_2As_2O_2$

atom	site symmetry	*x*	*y*	*z*	$U_i/U_e \times 100$
Sr	4e	0.000000	0.000000	0.41177(8)	0.22(5)
Mn	2a	0.000000	0.000000	0.00000	0.92(9)
Zn	4d	0.000000	0.500000	0.25000	0.97(13)
As	4e	0.000000	0.000000	0.16758(8)	0.10(4)
O	4c	0.000000	0.500000	0.00000	0.08(7)

[a] U_i/U_e is defined as one-third of the trace of the orthogonalized U_{ij} tensor.

Table 3. Selected Interatomic Distances (Å) and Bond Angle (degree) in $A_2MnM_2As_2O_2$ (A = Sr, Ba; M = Mn, Zn), Space Group *I*4/*mmm*

	$Sr_2MnZn_2As_2O_2$[a]	$Ba_2MnZn_2As_2O_2$[b]	$Sr_2Mn_3As_2O_2$[c]
A···O	2.63811(2)	2.7460(7)	2.625(2)
A···As	3.26982(2)	3.4053(11)	3.340(3)
A···M(4d)	3.65527(3)	3.7618(9)	3.739(6)
A···Mn(2a)	3.34804(2)	3.4666(6)	3.348(2)
As−M(4d)	2.57192(1)	2.5848(12)	2.574(1)
As···Mn (2a)	3.12680(3)	3.400(5)	3.191(7)
M(4d)−M(4d)	2.91539(2)	2.9923(2)	2.939
Mn(2a)−O	2.06149(1)	2.1158(1)	2.078
M(4d)−As−M(4d)	69.051(28)	70.84(4)	69.66

[a] Calculated from the powder neutron diffraction data. [b] Calculated from the powder neutron diffraction data (ref 18). [c] Calculated from the single-crystal X-ray diffraction data (ref 22).

transition metal toward oxygen, chalcogens, and pnicogens. Our goal in synthesizing these mixed-layer materials is to design and optimize their properties, which can be multifaceted, utilizing transition metal site control. For example, this strategy might be applied to the design of compounds with multiple properties, such as the recently reported ferromagnetic superconductor.[21]

In this paper, we present the synthesis and characterization of a new mixed-metal mixed-layer oxide, $Sr_2MnZn_2As_2O_2$, which is expected to have antiferromagnetic (AF) MnO_2^{2-} layers and diamagnetic $Zn_2As_2^{2-}$ layers. This compound is classified as a pnictide oxide[18,22−34] of the $Sr_2Mn_3As_2O_2$ structure type.[22] The

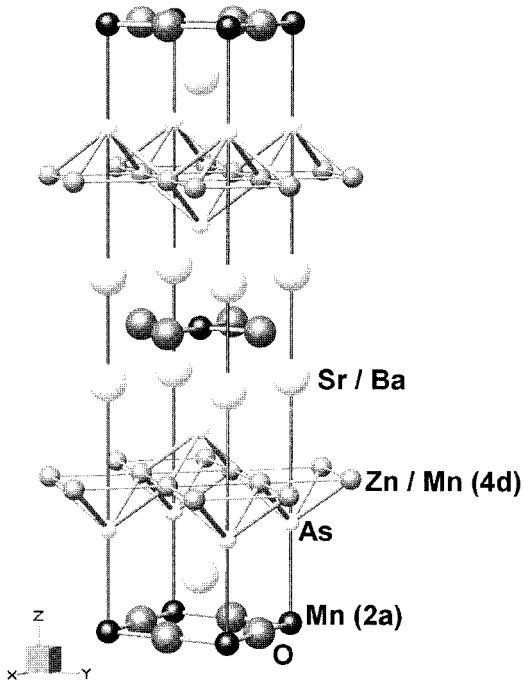

Figure 1. Perspective view of the structure of $A_2MnZn_2As_2O_2$ (A = Sr, Ba) showing alternating MnO_2^{2-} and $M_2As_2^{2-}$ (M = Mn, Zn) layers.

$Sr_2Mn_3As_2O_2$ structure has two independent transition metal layers: MnO_2^{2-} (square-planar M−O geometry observed in high-T_c cuprates and CMR manganites) and $Mn_2As_2^{2-}$ ($ThCr_2Si_2$-type[35] geometry observed in heavy fermion superconductors such as $CeCu_2Si_2$[36]). The Ba analogue, $Ba_2MnZn_2As_2O_2$, has been reported and was partially characterized by single-crystal X-ray diffraction, powder X-ray diffraction and powder neutron diffraction.[18] Field- and temperature-dependent magnetic susceptibility measurements were also made.[18] The results from these studies showed unambiguously the complete site selectivity of Mn in the oxide layer and Zn in the pnictide layer. Magnetic measurements indicate a possible transition below 38 K in $Ba_2MnZn_2As_2O_2$, which appears to be spin-glass-like in that the temperature-dependent zero-field-cooled (ZFC) and field-cooled (FC) susceptibilities diverge below this temperature.[37] The structure has body-centered tetragonal *I*4/*mmm* (no. 139) symmetry, and the sublattice of the Mn^{2+} ions is identical to those of the transition metals in K_2NiF_4-structure-type oxides such as high-T_c $La_{2-x}Ba_x$-

(21) Tallon, J.; Bernhard, C.; Bowden, M.; Gilberd, P.; Stoto, T.; Pringle, D. *IEEE Trans. Appl. Supercond.* **1999**, *9*, 1696.
(22) Brechtel, E.; Cordier, G.; Schäfer, H. *Z. Naturforsch. B* **1979**, *30*, 777.
(23) Stetson, N. T.; Kauzlarich, S. M. *Inorg. Chem.* **1991**, *30*, 3969.
(24) Brock, S. L.; Kauzlarich, S. M. *Inorg. Chem.* **1994**, *33*, 2491.
(25) Brock, S. L.; Kauzlarich, S. M. *Comments Inorg. Chem.* **1995**, *17*, 213.
(26) Brock, S. L.; Kauzlarich, S. M. *CHEMTECH* **1995**, *25*, 18.
(27) Brock, S. L.; Kauzlarich, S. M. *J. Alloys Compd.* **1996**, *241*, 82.
(28) Brock, S. L.; Raju, N. P.; Greedan, J. E.; Kauzlarich, S. M. *J. Alloys Compd.* **1996**, *237*, 9.
(29) Nientiedt, A. T.; Jeitschko, W.; Pollmeier, P. G.; Brylak, M. *Z. Naturforsch. B* **1997**, *52*, 560.
(30) Nientiedt, A. T.; Jeitschko, W. *Inorg. Chem.* **1998**, *37*, 386.
(31) Brock, S. L.; Hope, H.; Kauzlarich, S. M. *Inorg. Chem.* **1994**, *33*, 405.
(32) Cava, R. J.; Zandbergen, H. W.; Krajewski, J. J.; Siegrist, T.; Hwang, H. Y.; Batlogg, B. *J. Solid State Chem.* **1997**, *129*, 250.
(33) Adam, A.; Schuster, H.-U. *Z. Anorg. Allg. Chem.* **1990**, *584*, 150.
(34) Axtell, E. A., III; Ozawa, T.; Kauzlarich, S. M. *J. Solid State Chem.* **1997**, *134*, 423.
(35) Parthè, E.; Chabot, B. In *Handbook on the Physics and Chemistry of Rare Earths*; Gschneidner, K. A. Jr.; Eyring, L., Eds.; Elsevier: New York, 1984; Vol. 6, p 113.
(36) Steglich, F.; Aarts, J.; Bredl, C. D.; Lieke, W.; Meschede, D.; Franz, W.; Schäfer, H. *Phys. Rev. Lett.* **1979**, *43*, 1892.
(37) Mydosh, J. A. *Spin Glasses: An Experimental Introduction*; Taylor & Francis: London, 1993.

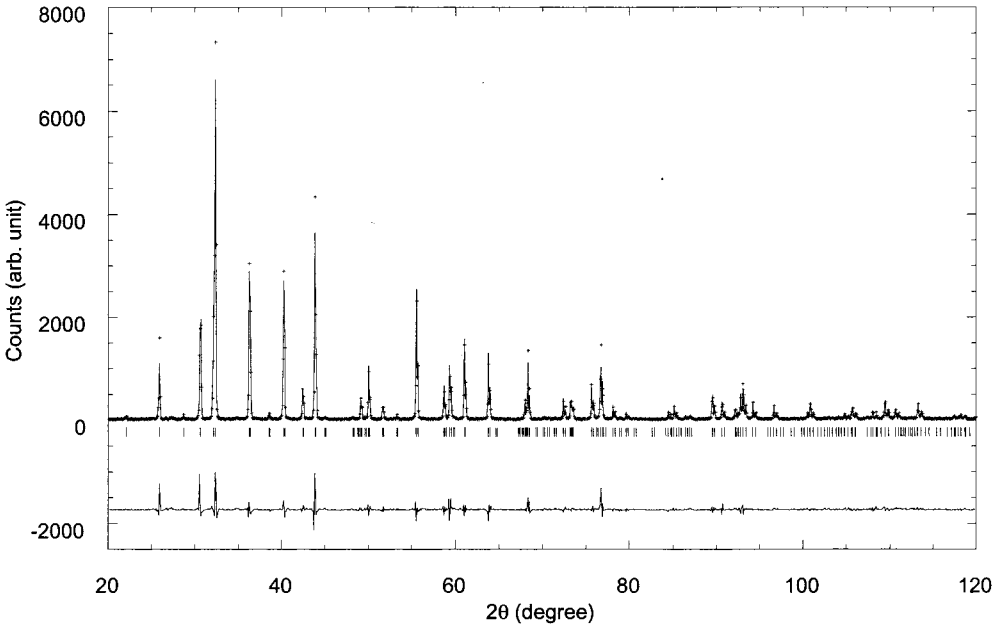

Figure 2. Rietveld refinement result for the powder X-ray diffraction data for $Sr_2MnZn_2As_2O_2$. The small points and solid line represent the experimental data and calculated pattern, respectively. The short vertical toggles represent allowed Bragg reflections, and the solid line at the bottom is the difference between the experimental and calculated data.

$CuO_{4-\delta}$,[38] incommensurate-charge-density-wave $La_2NiO_{4+\delta}$,[39] and charge-ordered $La_{2-x}Sr_xMnO_{4-\delta}$.[40−44] The physical properties of these transition metal oxides are very sensitive to the size of the alkaline earth ions, which determine in part the lattice parameters, and thus, one might also expect a similar sensitivity in the mixed-metal pnictide oxides $A_2MnZn_2As_2O_2$ (A = Ba, Sr). The new synthesized phase, $Sr_2MnZn_2As_2O_2$, is examined by powder X-ray and neutron diffraction and temperature-dependent magnetic susceptibility measurements. In addition, the magnetic structures of both the Sr and Ba analogues are investigated by low-temperature powder neutron diffraction, and structure−property relationships are explored by comparison with other members of this isostructural pnictide oxide family.

Experimental Procedures

Synthesis. The $Sr_2MnZn_2As_2O_2$ sample for X-ray diffraction and magnetic property characterization was prepared by solid-state sintering of a pressed pellet of the mixed powder of SrO, Mn, Zn, and As in the exact stoichiometric ratio. SrO was prepared from the thermal decomposition of $SrCO_3$ (J. Matthey, 99.99%) under vacuum (1000 °C, 24 h), and Mn (J. Matthey, 99.99%) was etched with 10 vol % HNO_3 in methanol and rinsed with acetone in order to remove any oxidized surface, transferred to a drybox, and preground before being mixed with other reagents. Zn (Fisher Scientific, 99.4%) and As (J. Matthey, 99.999%) were used as received. All of the reagents were ground in an agate mortar in a drybox under argon. The mixture was pressed into a pellet (approximately 1 g), placed in a predried alumina boat, and sealed in a fused-silica ampule under 0.2 atm of argon. The sample was then heated at a rate of 60 °C/h to 1000 °C and held at that temperature for 1 week. The product of the reaction was a dark gray solid that retained the original pellet shape. The yield of $Sr_2MnZn_2As_2O_2$, estimated from powder X-ray diffraction data, was quantitative, and no extra peaks were observed. However, a small amount of starting material was apparent at the end of the silica ampule and was found to be single crystals of Zn_2As_3 and other unidentified secondary phases. The product was observed to be stable in air for a long period of time (at least 6 months). An additional 5 g of sample was prepared for powder neutron diffraction in the same manner. A small amount of an unidentified light-gray-colored impurity was present in this sample, which appeared as a small extra peak in the powder neutron diffraction profile at around *d*-space ≈ 2.6 Å. The compound $Ba_2MnZn_2As_2O_2$ was prepared according to the published procedure.[18]

Powder X-ray Diffraction. Powder X-ray diffraction data were collected with a Siemens D500 X-ray diffractometer at room temperature using Cu K_α radiation. The powder diffraction pattern was scanned over 20−120° with a 0.02° step for 10 s/step. Rietveld refinement was performed utilizing the GSAS (General Structure Analysis System) software package.[45] The initial lattice parameters and atomic positions were taken from well-characterized $Sr_2Zn_3As_2O_2$ powder X-ray diffraction data.[27] The lattice parameters, background coefficients (power series in $q2n/n!$ and $n!/q2n$), preferred orientation parameters (spherical harmonic model[46,47]), atomic positions, isotropic thermal factors, and profile coefficients were refined. Results of the refinement are provided in Table 1.

Spallation Source Powder Neutron Diffraction. Powder neutron diffraction data were collected on the General Purpose Powder Diffractometer (GPPD) at the Intense Pulsed Neutron Source in order to analyze the transition metal site selectivity and occupancy. The sample was placed in a vanadium tube filled with helium gas, and time-of-flight data were collected at room temperature. Structure characterization was performed on the data from the ±148° detector banks using

(38) Bednorz, J. G.; Müller, K. A. *Z. Phys. B* **1986**, *64*, 189.
(39) Demourgues, A.; Weill, F.; Darriet, B.; Wattiaux, A.; Grenier, J. C.; Gravereau, P.; Pouchard, M. *J. Solid State Chem.* **1993**, *106*, 317.
(40) Tokunaga, M.; Miura, N.; Moritomo, Y.; Tokura, Y. *Phys. Rev. B* **1999**, *59*, 11151.
(41) Sternlieb, B. J.; Hill, J. P.; Wildgruber, U. C.; Luke, G. M.; Nachumi, B.; Moritomo, Y.; Tokura, Y. *Phys. Rev. Lett.* **1996**, *76*, 2169.
(42) Bao, W.; Chen, C. H.; Carter, S. A.; Cheong, S.-W. *Solid State Commun.* **1996**, *98*, 55.
(43) Bouloux, J. C.; Soubeyroux, J. L.; Daoudi, A.; LeFlem, G. *Mater. Res. Bull.* **1981**, *16*, 855.
(44) Moritomo, Y.; Tomioka, Y.; Asamitsu, A.; Tokura, Y. *Phys. Rev. B* **1995**, *51*, 3297.
(45) Larson, A. C.; Von Dreele, R. B. LANSCE, MS-H805; Los Alamos National Laboratory: Los Alamos, NM, 1990.
(46) Bunge, H. J. *Texture Analysis in Material Science*; Butterworths: London, 1982.
(47) Popa, N. C. *J. Appl. Crystallogr.* **1992**, *25*, 611.

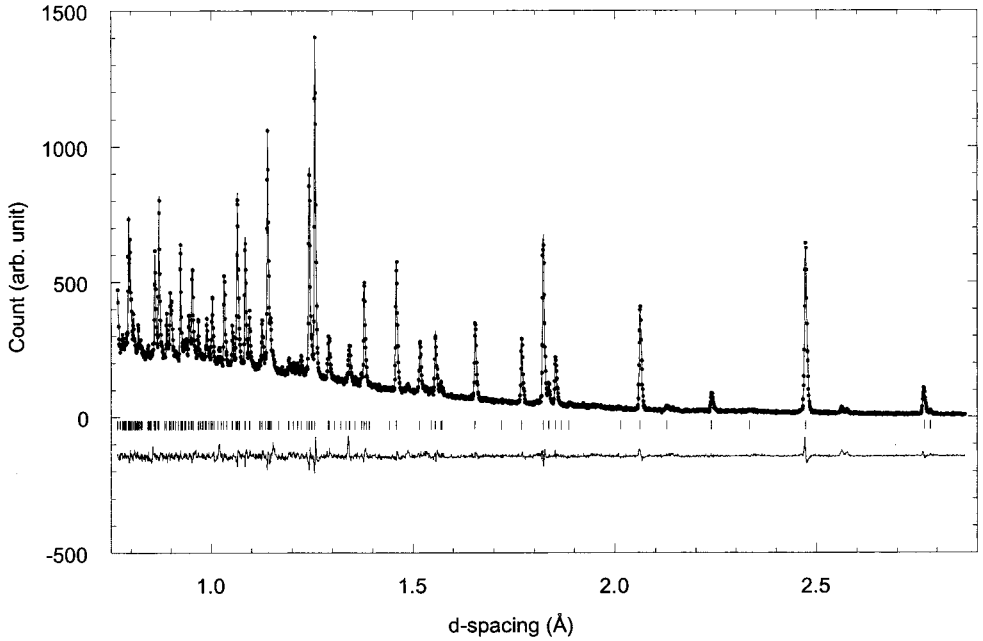

Figure 3. Rietveld refinement result for the powder neutron diffraction (GPPD) data for $Sr_2MnZn_2As_2O_2$. The small points and solid line represent the experimental data and calculated pattern, respectively. The short vertical toggles represent allowed Bragg reflections, and the solid line at the bottom is the difference between the experimental and calculated data.

the GSAS software package.[45] Initial crystallographic parameters for this refinement were taken from the previously performed Rietveld refinement results on the powder X-ray diffraction data of the same phase. In addition to the parameters refined for powder X-ray diffraction data, the transition metal site [2a (0 0 0) and 4d (0 0.5 0.25) in *I*4/*mmm* symmetry] occupancies were refined, taking advantage of the different scattering lengths of Mn (-0.373×10^{-12} cm) and Zn (0.568×10^{-12} cm). The refinement was performed using the following models: both 2a and 4d sites occupied by Mn, both 2a and 4d occupied by Zn, 2a by Mn and 4d by Zn, and a Mn−Zn solid solution.

Magnetic Susceptibility Measurements. Temperature-dependent dc-magnetic susceptibility was measured on a Quantum Design SQUID magnetometer. The sample was ground into powder and sealed under vacuum in a fused-silica tube designed to provide negligible background. Magnetization versus temperature data were collected in a 5-kOe field over the temperature range of 5−300 K for both ZFC and FC measurements. The applied field of 5 kOe was chosen so as to compare these results with those previously published for $Sr_2Mn_3As_2O_2$[27] and $Ba_2MnZn_2As_2O_3$.[18]

Reactor Source Powder Neutron Diffraction. The magnetic structures of $Sr_2MnZn_2As_2O_2$ and $Ba_2MnZn_2As_2O_2$ were investigated by powder neutron diffraction on the High-Resolution Powder Diffractometer (HRPD) at the DUALSPEC of Chalk River Laboratories. Diffraction data were acquired at 100 and 25 K for $Sr_2MnZn_2As_2O_2$ and at 50, 40, 30, 20, 15, and 4 K for $Ba_2MnZn_2As_2O_2$, with a neutron beam wavelength of $\lambda = 2.3692$ Å. The samples were sealed in vanadium tubes with indium gaskets, and the temperature was controlled by a helium closed-cycle cryostat. The magnetic and structural Rietveld refinement of the data for $Ba_2MnZn_2As_2O_2$ was performed using FULLPROF[48,49] and a locally written program for fitting the asymmetric Warren line shape.

Results and Discussion

The crystal structure of $Sr_2MnZn_2As_2O_2$ is shown in Figure 1. This compound crystallizes in the tetragonal space group *I*4/*mmm* and, as already mentioned, consists of a 1:1 intergrowth of alternating MnO_2^{2-} and $Zn_2As_2^{2-}$ layers separated by Sr^{2+}. The MnO_2^{2-} layers show square-planar coordination of Mn^{2+} (2a site) with oxygen, whereas in the $Zn_2As_2^{2-}$ layers, Zn^{2+} (4d site) has tetrahedral coordination with As^{3-}, forming $ZnAs_{4/4}^{-}$ square-pyramidal units. These units are arranged in an edge-shared manner, with alternating up and down orientation of the square pyramid. Figures 2 and 3 show the Rietveld refinement results for the powder X-ray and neutron diffraction data, respectively. The powder X-ray diffraction fit is not as good as that resulting from the powder neutron diffraction data. The lower quality of fit for powder X-ray diffraction is attributed to the preferred orientation that is clearly visible in Figure 2. The lattice parameters obtained from X-ray diffraction are $a = 4.126277(31)$ Å and $c = 18.67105(17)$ Å, in good agreement with those from neutron diffraction data, $a = 4.122979(26)$ Å and $c = 18.65868(21)$ Å (Table 1). These parameters are intermediate between those of the all-Mn compound $Sr_2Mn_3As_2O_2$[27] and the all-Zn compound $Sr_2Zn_3As_2O_2$.[24] Atomic positions, refinement results, and selected interatomic distances from the neutron diffraction data from GPPD are summarized in Tables 2 and 3. Rietveld analysis of the powder neutron diffraction data shows that the oxide layers are practically fully occupied by Mn^{2+} [99.6(4)%], as expected. However, the pnictide layer site occupancies by Zn^{2+} and Mn^{2+} are found to be 94.0(5)% and 6.0(5)%, respectively. Although this is only a small amount of Mn in the pnictide layer, the fact that there is any amount greater than 1% is surprising. Rietveld refinement of neutron data for the Ba analogue phase showed complete site selectivity with Mn only in the oxide layer and Zn only in the pnictide layers.[18] The difference between the Sr and Ba analogues might be due to preparative conditions. In case of the Sr compound, unlike the Ba analogue, significant amounts of Zn_2As_3 separated from the starting materials by gas-phase

(48) Wiles, D. B.; Young, R. A. *J. Appl. Crystallogr.* **1981**, *14*, 149.
(49) Rodríguez-Carvajal, J. *Physica B* **1993**, *192*, 55.

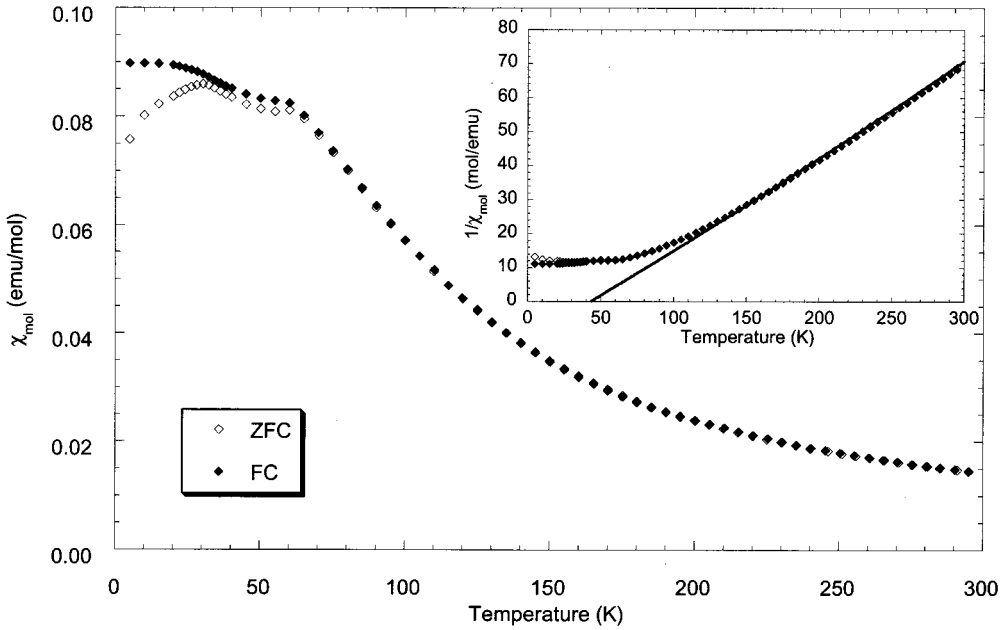

Figure 4. Zero-field-cooled (ZFC) and field-cooled (FC) temperature-dependent dc-magnetic susceptibilities for $Sr_2MnZn_2As_2O_2$ measured at 5 kOe. The inset shows the Curie−Weiss plot and a positive θ_{CW} value.

diffusion. The lack of full occupancy in the pnictide layer by Zn might thus be a result of this loss of Zn during preparation.

Figure 4 shows the result of ZFC and FC dc-magnetic susceptibility measurement under a 5-kOe applied field. ZFC data are fit to a modified Curie−Weiss law, $[\chi = C/(T - \theta_{CW}) + \chi_o]$ over the temperature range 170−300 K. This fit gives $\chi_o = -9(2) \times 10^{-4}$ and $C = 3.89(7)$, which provides $\mu_{eff} = 5.56(1)\mu_B$. This result corresponds well with the expected spin-only ($S = {}^5/_2$) effective moment of $5.91\mu_B$ for high-spin Mn^{2+}. Much more surprising is the positive value for the Weiss constant, $\theta_{CW} = 43(2)$ K (inset). This value is quite different from that of the Ba analogue, for which $\theta_{CW} = -51(5)$ K, consistent with a net AF intralayer coupling.[18] This observation should be verified by further measurements at higher temperatures, but assuming that the positive Weiss constant for the Sr analogue is correct, this suggests that there is significant ferromagnetic interlayer coupling, which might result from the short interlayer distance. In these materials, AF coupling between the nearest MnO_2^{2-} layers is expected to cancel based on symmetry arguments, i.e., because of the I-centered stacking sequence. Nonetheless, long-range order is frequently observed for K_2NiF_4-structure materials and is attributed to the coupling of each layer to the next-nearest layer, which is more favorable than the nearest layer.[50] In such layered antiferromagnets, there is usually a significant temperature range over which the susceptibility exhibits signs of the short-range intralayer AF correlations in the form of a broad maximum. The ZFC data of Figure 5 show no such feature for either the Sr or Ba materials; therefore, the two-dimensional Heisenberg AF model is not appropriate for these compounds.[51−53] An effort was made to find evidence for a transition temperature (T_c) to a long-range-ordered state by plotting $d(\chi T)/dT$ (proportional to the heat capacity) versus temperature and finding the maximum point.[54] Although such maxima can be found at 55 and 38 K for the Sr and Ba materials, respectively, the results of the neutron diffraction studies to be discussed shortly indicate that no true long-range-ordered state is found in either case.

The magnetic ground states for $Sr_2MnZn_2As_2O_2$ and the Ba analogue are more likely to be of the spin-glass-type, consistent with the observed divergence in the ZFC and FC susceptibilities below 55 and 38 K, respectively, which are thus better assigned as spin freezing temperatures, T_F.[37] Similar behavior is also observed for the Mn (2a) sublattice in $Sr_2Mn_3As_2O_2$.[27]

More definitive information on the nature of the ground state can be obtained from low-temperature neutron diffraction studies. Beginning with $Ba_2Zn_2MnAs_2O_2$, Figure 6a, the data at 4 K are refined using a three-phase model including the Ba-phase crystal structure and the crystal and magnetic structures of a MnO impurity phase. The only significant features in the difference plot are peaks at approximately 27° and 23° in 2θ. The peak at around 27° is indexed as the $({}^1/_2\ {}^1/_2\ {}^1/_2)$ MnO magnetic reflection. The peak at around 23° has an asymmetric Warren-like profile,[55] and it is indexed as the (1 0 0) magnetic reflection of $Ba_2MnZn_2As_2O_2$ with the magnetic cell, $a_{mag} = \sqrt{2}a$. The presence of a Warren-like peak indicates two-dimensional short-range order. Using the Warren line-shape function, the diffraction data were fit to extract an effective correlation length for the magnetic interactions. The fit included a small Gaussian feature in the tail of the function at about 25° in 2θ, and the result is shown in Figure 6b. As can be seen in Figure 7, the correlation length increases sharply below about 30 K, consistent with the observed temperature-dependent magnetic susceptibility, and attains a maximum value of ~250 Å

(50) de Jongh, L. J.; Miedema, A. R. *Adv. Phys.* **1974**, *23*, 1.
(51) Lines, M. E. *J. Phys. Chem. Solids* **1970**, *31*, 101.
(52) Rushbrooke, G. S.; Wood, P. J. *Mol. Phys.* **1958**, *1*, 257.
(53) Rushbrooke, G. S.; Wood, P. J. *Mol. Phys.* **1963**, *6*, 409.
(54) Fisher, M. E. *Philos. Mag.* **1962**, *17*, 1731.
(55) Warren, B. E. *Phys. Rev.* **1941**, *59*, 693.

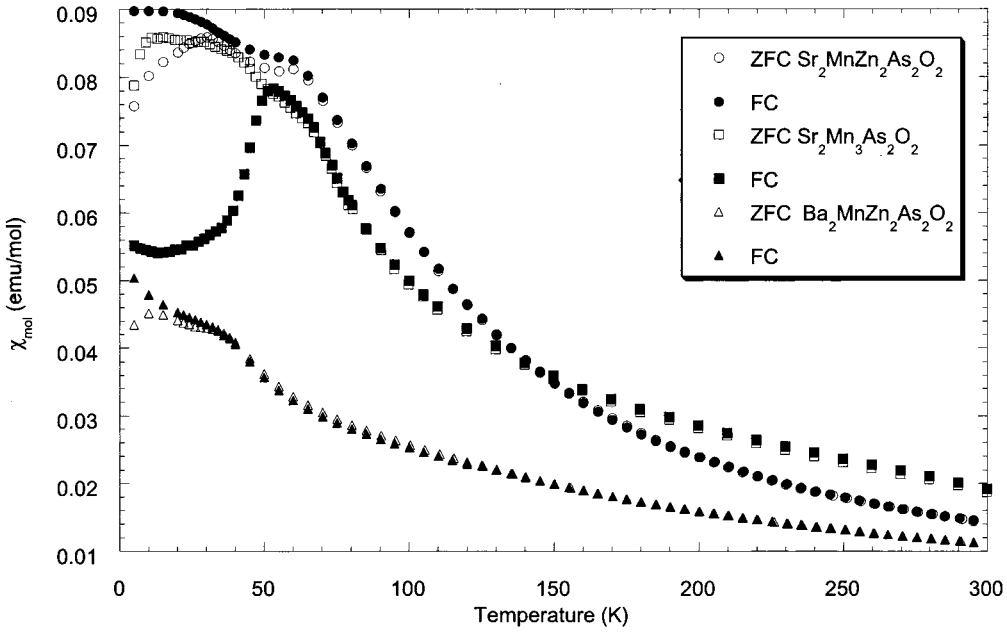

Figure 5. Zero-field-cooled (ZFC) and field-cooled (FC) temperature-dependent dc magnetic susceptibilities for $A_2MnM_2As_2O_2$ (A = Sr, Ba; M = Mn, Zn) measured at 5 kOe.

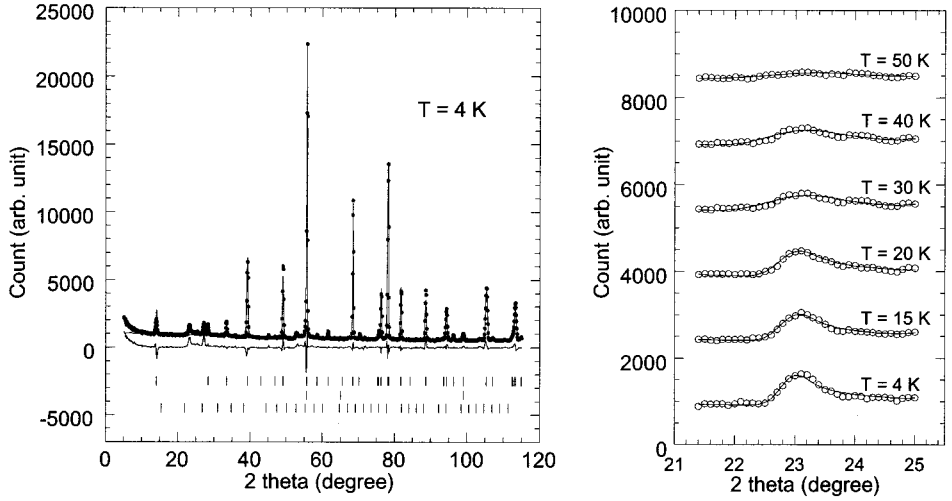

Figure 6. (a) Rietveld refinement result for the powder neutron diffraction (DUALSPEC) data for $Ba_2MnZn_2As_2O_2$ at 4 K. The small points and solid line represent the experimental data and calculated pattern, respectively. The short vertical toggles represent allowed Bragg reflections for $Ba_2MnZn_2As_2O_2$, Bragg reflections for MnO, and magnetic reflection for MnO from top to the bottom. The solid line at the bottom is the difference between the experimental and calculated data. (b) Powder neutron diffraction profiles at 4, 15, 20, 30, 40, and 50 K.

at 4 K. However, true long-range order is never established. The increase in correlation length might be an indication of the onset of three-dimensional interactions, but true long-range order is never established.[56] The temperature dependence of the lattice parameters was also analyzed. The result (Table 4) shows that the lattice parameter *a* decreases linearly with temperature over the range of 60−4 K and that *c* decreases linearly over the range of 60−30 K; below 30 K, there is no change. This might be interpreted as a structural distortion at T_F.

The results for $Sr_2MnZn_2As_2O_2$ offer a significant contrast. Figure 8 shows the difference plot for 100 and 2.5 K, which is featureless apart from the artifacts due to the shift in the cell constants. There is certainly no sign of the Warren peak, which would be expected near 23°, nor indeed is there any evidence for either short- or long-range magnetic order in the 2θ range investigated.

The factors that select the spin glassy state over the ordered AF state for the Mn (2a) sites in these materials are not yet clear, but there might be a correlation with the *c*-axis lattice constant. Consider the following four compounds, relevant properties for which are collected in Table 5: (1) $Sr_2Mn_3Sb_2O_2$, (2) $Ba_2MnZn_2As_2O_2$, (3) $Sr_2Mn_3As_2O_2$, and (4) $Sr_2MnZn_2As_2O_2$. The *c*-axis lattice constant decreases in the order listed, and the magnetic properties of the Mn (2a) sublattice show systematic changes. Recall that for the two all-Mn phases, the Mn (4d) sublattice orders independently above 300 K. Phase 1 is the only one for which the Mn (2a) sublattice orders

(56) de Jongh, L. J. In *Magnetic Properties of Layered Transition Metal Compounds*; de Jongh, L. J., Ed.; Kluwer Academic Publishers: Dordrecht, The Netherlands, 1990; p 19.

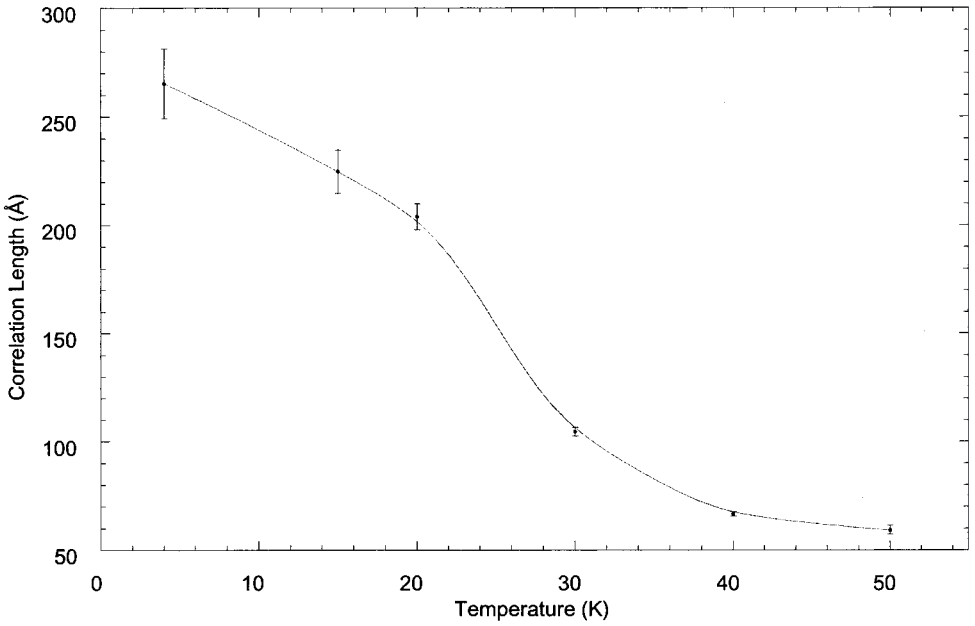

Figure 7. Correlation length as a function of temperature for $Ba_2MnZn_2As_2O_2$.

Table 4. Rietveld Refinement Result of the Powder Neutron Diffraction Data for $Ba_2MnZn_2As_2O_2$

	4 K[a]	15 K	20 K	30 K	40 K	50 K	60 K
a (Å)	4.2165(1)	4.2176(1)	4.2177(1)	4.2178(1)	4.2180(1)	4.2182(1)	4.2184(1)
c (Å)	19.3985(7)	19.4042(8)	19.4042(8)	19.4041(8)	19.4054(8)	19.4060(8)	19.4074(8)
R_p (%)	6.11	5.12	5.13	4.97	4.90	4.92	4.65
R_{wp} (%)	8.63	7.37	7.26	7.14	7.11	7.19	6.84
χ^2	7.86	6.35	6.18	5.96	5.88	5.98	5.46
Bragg R factor	6.13	5.23	5.18	5.13	4.81	4.99	5.05
R−F factor	6.19	6.34	5.80	5.88	5.35	5.64	5.81

[a] The 4 K data set was taken under different instrumental set up, and the wavelength calibration is inaccurate.

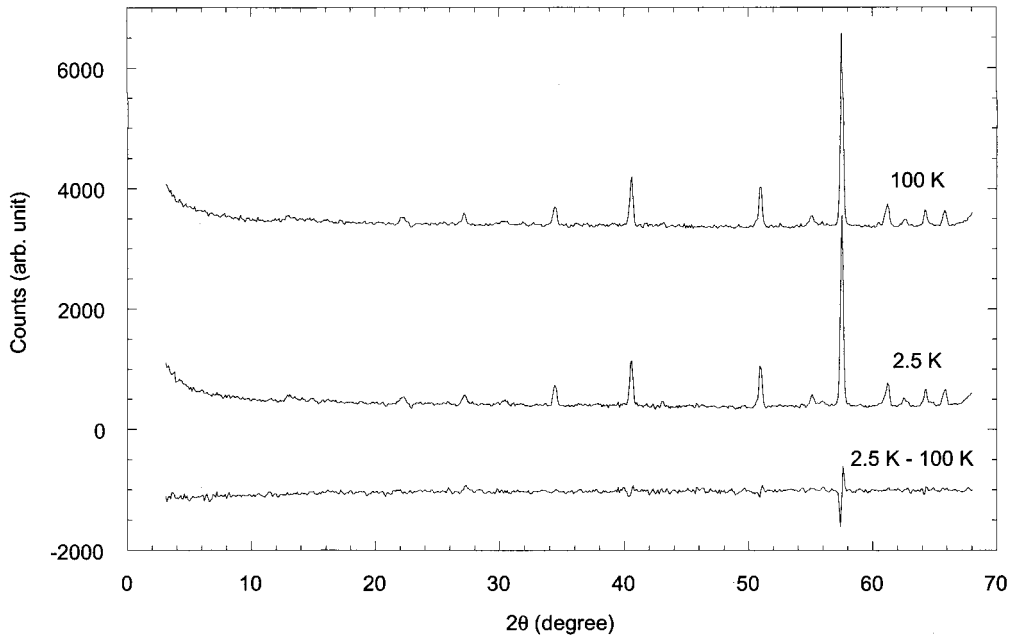

Figure 8. Difference plot of the neutron powder data for $Sr_2MnZn_2As_2O_2$, 2.5−100 K, obtained from DUALSPEC.

at 65 K. Compounds 2 and 3 show only short-range, two-dimensional AF correlations, and 4 shows no clear indication of order of any type. These systematic differences might be connected with an increasing level of ferromagnetic correlations as a function of decreasing *c*-axis or interlayer separation, and there is some support for this idea from the susceptibility data, but more work needs to be done to verify or refute this hypothesis.

Conclusions

The new compound $Sr_2MnZn_2As_2O_2$ exhibits complete 2a site occupation by Mn and nearly complete 4d site occupation by Zn. The magnetism of $Sr_2MnZn_2As_2O_2$ is

Table 5. Summary of Magnetic and Crystallographic Data for the Compounds $A_2MnM_2(As, Sb)_2O_2$ (A= Ba, Sr; M = Mn, Zn)

	T_c (K)	θ_{CW} (K)	T_F (K)	a (Å)	c (Å)
$Sr_2Mn_3Sb_2O_2$	65	−	−	4.2679(5)	20.159(3)
$Ba_2MnZn_2As_2O_2$[a]	−	−51(5)	38	4.23369(4)	19.5087(7)
$Sr_2Mn_3As_2O_2$[b]	−	−	51	4.1459(6)	18.856(2)
$Sr_2MnZn_2As_2O_2$	−	+43(2)	55	4.12298(3)	18.6587(2)

[a] Data adapted from ref 18. [b] Data adapted from ref 27.

similar to that of the isostructural oxy-chalcogenide compounds $Sr_2Cu_2MO_2S_2$ (M = Mn, Zn).[13,14] All of the oxy-chalcogenide compounds also show spin-glass-like behavior and fail to fit to the two-dimensional Heisenberg AF model. One hypothesis is that this spin-glass-like behavior and the lack of both two- and three-dimensional magnetic order in $Sr_2MnZn_2As_2O_2$ is due to the small intra- and interlayer distances in this material. Verification of this hypothesis requires further investigations such as a pressure effect analysis on the structure and magnetism of the isostructural pnictide oxide systems $A_2MnM_2Pn_2O_2$ (A = Sr, Ba; M = Mn, Zn; Pn = Sb, Bi).

Acknowledgment. We thank Stephanie L. Brock for her contribution to the early part of this investigation; Robert N. Shelton for the use of the SQUID magnetometer and X-ray diffractometer; Peter Klavins for assistance in instrumentation; James W. Richardson, Jr. for the powder neutron diffraction data acquisition at IPNS; and David J. Webb for the useful discussions on magnetism. This research is supported by NSF DMR-9803074 and the Natural Sciences and Engineering Research Council of Canada. Also, this work has benefited from the use of the Intense Pulsed Neutron Source at Argonne National Laboratory. This facility is funded by the U.S. Department of Energy, BES-Materials Science, under Contract W-31-109-Eng-38. We also acknowledge the Neutron Program for Materials Research of the National Research Council of Canada, which operates the DUALSPEC instrument at the Chalk River Nuclear Laboratory.

CM000743J